THE JOURNAL OF PHYSICAL CHEMISTRY C
A JOURNAL OF THE AMERICAN CHEMICAL SOCIETY

pubs.acs.org/JPCC

Article

Influence of Alkyl Chain Variation on Cocrystal Formation and Molecular Charge Transfer in DIP:Perylene Diimide Binary Systems

Nadine Rußegger, Hongwon Kim, Jakub Hagara, Oleg Vladimirov, Timo Eberle, Ivan Zaluzhnyy, Alexander Gerlach, Alexander Hinderhofer,* Wolfgang Brütting,* and Frank Schreiber*

Cite This: J. Phys. Chem. C 2023, 127, 11128−11137

Read Online

ACCESS | Metrics & More | Article Recommendations | Supporting Information

ABSTRACT: We present a comprehensive investigation of cocrystal formation and charge transfer effects in weakly interacting organic semiconductor mixtures. As a model system, we choose diindenoperylene (DIP) as a donor molecule and several perylene diimide derivatives (PDI) as acceptor molecules that differ in the *n*-alkyl side chain in the imide position and in the cyano (CN) group in the bay position. We identified the optimized side groups for the acceptors in thin films with the donor DIP concerning the mixing behavior and molecular charge transfer (CT) effects. The two systems, which form a well-defined cocrystal and show excited-state charge transfer effects, are DIP:PTCDI-C_3 with an *n*-propyl side chain and DIP:PTCDI-C_8-CN_2 with incorporated cyano groups. Important for the mixing behavior and the charge transfer effects with DIP are the intermolecular interactions of the pure perylene diimide derivatives and the orientation of these molecules on the substrate (SiO_2). For the DIP:PTCDI-C_3 system, a sharp CT peak in absorption with a well-defined CT energy is observed. In contrast, the DIP:PTCDI-C_8-CN_2 mixed films show a broad CT band in absorption and two different CT energies. The mixing behavior and charge transfer effects with DIP are strongly influenced by the structure of the acceptors, which are easily chemically tunable in the desired way.

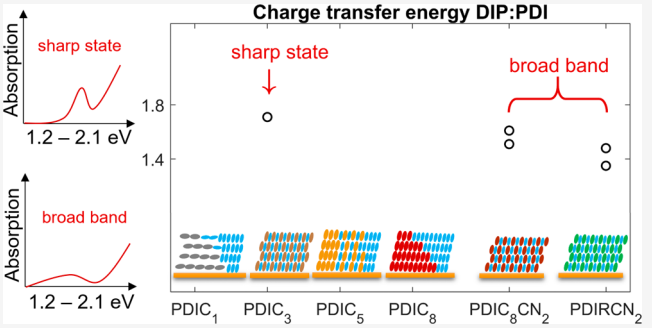

INTRODUCTION

Organic small molecules are an attractive alternative to inorganic materials, which are widely used in organic optoelectronic devices such as organic photovoltaic (OPV) cells and organic light-emitting diodes (OLEDs). In such devices, one of the fundamental processes relies on molecular charge transfer (CT), which takes place at the interface of donor and acceptor molecules or in a molecular mixed system.[1−3] The tuning of the interactions and CT effects at these interfaces involves rather rich physics and chemistry and comes with many subtleties.[4,5] Depending on the strength of molecular interactions, molecular charge transfer can be divided into several different categories. For the limiting case of weakly bound organic small molecules, a partial charge transfer on average from the donor to the acceptor is expected.[6−8] A great impact on charge transfer effects has in this context the morphology and intermixing on the molecular level in bulk heterojunction thin films.[9−12]

One group of organic small molecules, which are widely used as electron donors and acceptors in organic electronic devices, especially for organic field effect transistors (OFETs),[13] are perylene diimide derivatives.[14−18] Due to their relatively strong electron affinities, they are very promising *n*-type organic materials. They show excellent chemical and thermal stabilities, high light absorption capabilities, and high fluorescence quantum yields.[19,20] Through the incorporation of different side groups, PDIs can easily be chemically modified to suit solubility, photophysical, or electron-bearing demands and be very suitable for organic electronic applications.[20−22] They are structurally well-defined, and due to the tailoring of the charge-transport properties upon changing the substituents on the imide or the bay position of the perylene backbone,[14,21,23,24] they can serve as an acceptor model system. However, so far there are only few publications on donor−acceptor thin film systems of PDI derivatives with organic small donor molecules.[25−28]

Despite intense research on CT effects in organic blends, there is still no theory with predictive power for these rather complex systems. Therefore, systematic experimental investigations of new material combinations are required. We present a comprehensive study of structure-dependent mixing behavior and charge transfer effects in different organic small molecule donor−acceptor systems. As acceptor materials different perylene diimide derivatives were chosen, which differ in the

Received: October 26, 2022
Revised: May 14, 2023
Published: June 6, 2023

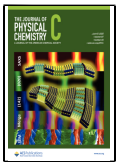

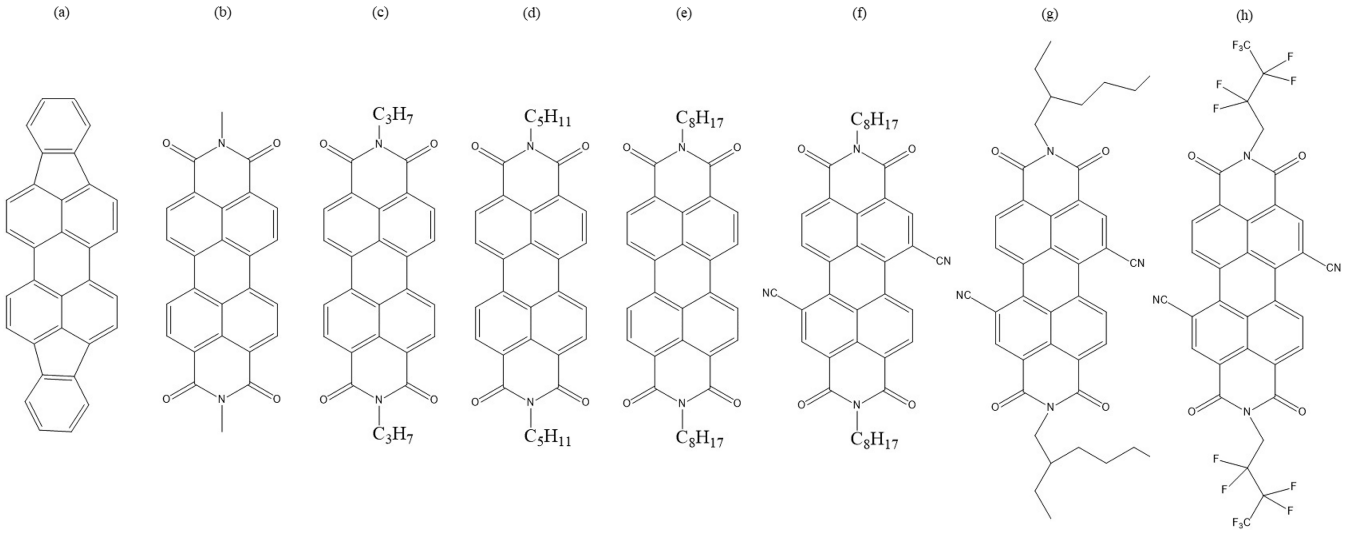

Figure 1. Overview of the studied compounds: (a) donor DIP, different perylene diimide acceptors, (b) PTCDI-C_1, (c) PTCDI-C_3, (d) PTCDI-C_5, (e) PTCDI-C_8, (f) PTCDI-C_8-CN_2, (g) PDIR-CN_2, and (h) PDIF-CN_2.

length of the *n*-alkyl side chain in the imide position (PTCDI-C_1, PTCDI-C_3, PTCDI-C_5, and PTCDI-C_8) and in the cyano group in the bay position (PTCDI-C_8−CN_2) (Figure 1). In previous studies it was shown that alkyl, branched, and fluorinated side chains and electron-withdrawing side groups can alter the molecular packing and morphology of the deposited thin films.[19,21,24,29] By varying the *n*-alkyl side chain and by incorporating cyano groups, the different mixing behaviors and the influence on possible charge transfer effects can be investigated in such systems. As donor molecule diindenoperylene (DIP; Figure 1) was chosen, which is known for its applications in organic electronics. DIP is used as a donor molecule in OPV devices and as a *p*-type organic semiconductor in OFETs.[30,31] The growth behavior of DIP in thin films is well established.[32−35] DIP crystallizes in a herringbone structure motif and is arranged in a standing-up orientation if grown under suitable conditions (T > 300 K) on SiO_2 substrates.[33,34,36] With its structure and size, the donor molecule has a similar shape as the perylene diimide core and does not contain any sterically hindering side groups. Therefore, DIP is a perfect donor molecule for the different perylene diimide derivatives. It was shown that DIP can form a well-defined cocrystal with a partial charge transfer with the two perylene diimide derivatives PDIR-CN_2 and PDIF-CN_2 (Figure 1).[8,37]

In this study, we examine the optimization of the side groups for perylene diimide acceptors with the donor DIP in thin films prepared by organic molecular beam deposition (OMBD)[36,38−40] regarding structural morphology and charge transfer effects. We discuss the different mixing behaviors for the different PDI:DIP systems studied by grazing-incidence wide-angle X-ray scattering (GIWAXS). We demonstrate the maximization of intermixing and cocrystal formation regarding different side chains of the acceptor molecules. Combining the structural analysis with optical spectroscopy, we investigate the different systems of excited-state charge transfer effects studied by absorption and emission spectroscopy. Correlations between structural morphology and charge transfer effects were established depending on the chain length and their configuration within the different perylene diimide:DIP mixed systems.

METHODS

PTCDI-C_1, PTCDI-C_3, PTCDI-C_5, and PTCDI-C_8 were bought from Sigma-Aldrich (purity of 98%). PTCDI-C_8-CN_2 was bought by Flexterra, DIP from Stephan Hirschmann, University of Stuttgart, and used as received. The samples were prepared by OMBD under ultrahigh vacuum ($p = 2 \times 10^{-10}$ mbar).[36,38,39] Three different substrates were used for the different structural and optical investigations: a silicon 111 wafer with a native oxide layer of 2 nm, a transparent glass wafer, and a glass wafer that was roughened at the backside. The substrates were cleaned with acetone and isopropyl alcohol in an ultrasonic bath each for 10 min and degassed overnight in the chamber before film preparation. The substrates were kept at a constant temperature of 293 or 423 K during film growth. Mixed thin films were prepared by coevaporation of the donor DIP and the different perylene diimide derivatives with a mixing ratio of 1:1. The nominal thicknesses of about 20 nm and growth rates of about 0.2 nm min^{-1} in total were controlled by a quartz crystal microbalance (QCM) during film growth and calibrated by X-ray reflectivity (XRR). For the mixed layer devices, we used indium−tin oxide (ITO)-coated glass substrates. A polymeric hole injection layer (HIL 1.3) was spin-coated from an aqueous solution and annealed at 398 K for 30 min. As the active layer, the organic molecules were evaporated under vacuum (20 nm DIP/50 nm equimolar DIP:PDI/20 nm PDI). Onto an exciton blocking layer of bathocuproine (BCP, 5 nm), aluminum (100 nm) was thermally deposited through a shadow mask.

For structural analysis, XRR was measured with a GE Inspection Technologies XRD 3003 TT X-ray diffraction system using Cu $K_{\alpha 1}$ radiation (λ = 1.5406 Å). XRR data fitting was done with GenX[41] by means of the Parratt formalism.[42] GIWAXS measurements were performed at the beamlines P03 and P08 of the German Electron Synchrotron DESY (Hamburg, Germany) using X-rays with a wavelength of 0.9686 and 0.6888 Å. UV/vis/NIR spectra were acquired using a Varian Cary 50 spectrometer in the wavelength range of 200−1100 nm at normal incidence. Photoluminescence (PL) spectra were collected using a Horiba Jobin Yvon Labram HR 800 spectrometer with a CCD 1024 × 256 detector. For PL excitation a Nd:YAG laser with a wavelength of 532 nm was used. Temperature-dependent PL spectra were determined with

https://doi.org/10.1021/acs.jpcc.2c07524
J. Phys. Chem. C 2023, 127, 11128−11137

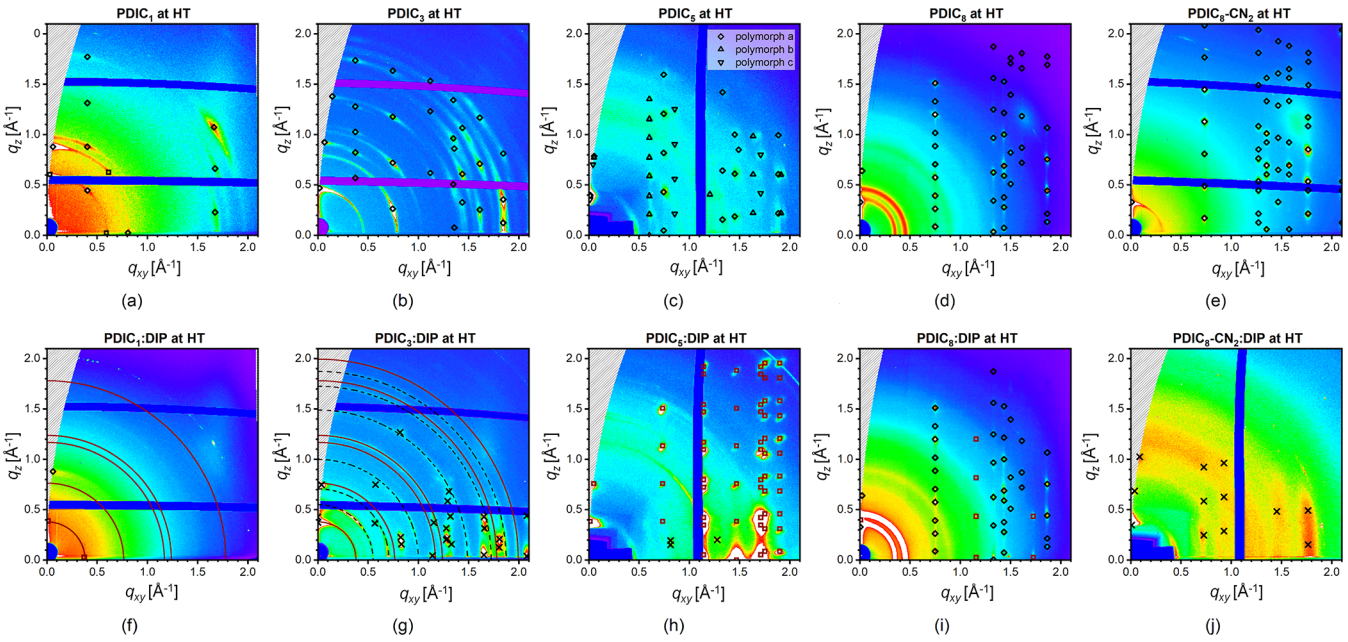

Figure 2. GIWAXS data (150 °C deposition temperature): (a) $PDIC_1$, (b) $PDIC_3$, (c) $PDIC_5$, (d) $PDIC_8$, (e) $PDIC_8$-CN_2, (f) DIP 1:1 $PDIC_1$, (g) DIP 1:1 $PDIC_3$, (h) DIP 1:1 $PDIC_5$, (i) DIP 1:1 $PDIC_8$, and (j) DIP 1:1 $PDIC_8$-CN_2 (the donor is marked in violet, the acceptor is marked with black triangles or squares for the different phases and black crosses indicate the mixed phase).

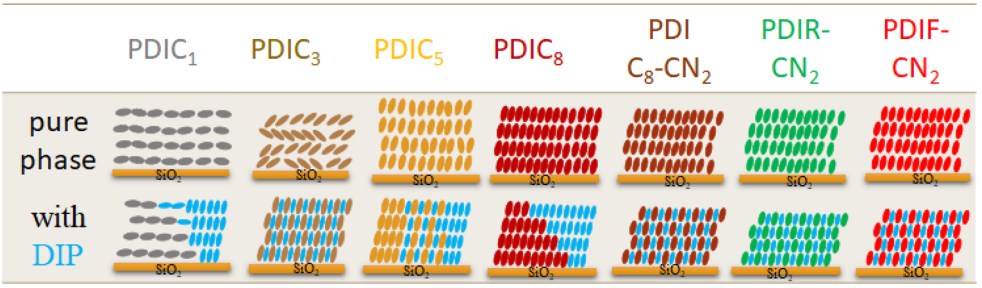

Figure 3. Schematic overview of the growth behavior for the different pure PDI derivatives and the mixing behavior with the donor DIP at high substrate temperature (the donor is colored in blue and the acceptors in the respective colors of their pure phases).

a CryoVac cooling system with liquid helium in the range from 293 to 15 K.[43] Electroluminescence (EL) measurements were carried out by using a CCD camera (PyLoN:100BR eXcelon, Princeton Instruments) coupled with a spectrometer (SP2300i, Princeton Instruments) under a dc voltage driven by a Keithley source meter (applied bias voltage of 3.5 V). Incident-photon-to-current efficiency (IPCE) was performed using a halogen lamp and a monochromator (Omni-λ300, Zolix Instruments Co., Ltd.), which allows measurements in the range from 350 to 1100 nm in steps of 1 nm.

RESULTS AND DISCUSSION

Structural Characterization. First, we study the thin-film structure of PDI:DIP mixtures and its dependence on side chain length in the imide position as well as the incorporation of cyano-groups in the bay positions of the acceptor. Such modifications of the molecular structure have a significant impact on the packing motif of both the pure and mixed film structures. Specifically, we investigate if the respective thin films exhibit phase-separation or form a solid solution. An overview of the GIWAXS data of different pristine perylene diimide derivatives and the mixtures with the donor DIP is shown in Figures 2, S4, and S5.

Depending on the length of the *n*-alkyl chains in the imide position, the various pristine perylene derivatives create different thin film structures, as shown in the GIWAXS patterns (Figure 2a–e).[16,44] For short alkyl chains (up to three C atoms), the molecules lie down with their long molecular axes close to parallel to the substrate surface (Figure 2a) and form the well-known herringbone structure.[45,46] With increasing length of the *n*-alkyl side chain, the orientation changes to a more upright conformation, and the molecules assume the offset-stacked geometry, where neighboring molecules are shifted relative to each other (Figure 2c–e).[15,47−49] An exception to this behavior is PTCDI-C_3 ($PDIC_3$). The compound grows in an intermediate form between the aforementioned orientations and geometries in thin films.[50] With this alkyl chain length, the perylene diimide molecules are oriented to a more standing-up conformation on the silicon substrate, and a more offset-stacked orientation is established (Figure 2b). An overview of the growth behavior for the individual pure PDI derivatives at high substrate temperature is shown in Figure 3. The different unit cell parameters are given in Table S1.

Important for the comparison of these pristine films is the increasing crystallinity with increased *n*-alkyl chain length in the imide position, since the longer *n*-alkyl chain can be arranged in

https://doi.org/10.1021/acs.jpcc.2c07524
J. Phys. Chem. C 2023, 127, 11128−11137

an energetically favorable conformation to achieve a higher packing density. We speculate that the additional van der Waals forces between the longer *n*-alkyl side chains lead to more favorable intermolecular $\pi-\pi$ stacking between the perylene diimide molecules, the so-called fastener effect.[51−54] This implies that the orientation of the perylene diimide derivative molecules in the thin film structure depends on the *n*-alkyl chain length and also influences the mixing behavior with the donor molecule DIP.

The mixing behavior of the organic small molecules in this study is considered in terms of a nearest-neighbor interaction model (eq 1), which is similar to the Flory−Huggins solution theory.[9] The main driving force is the difference between the intermolecular interaction of similar (W_{AA} or W_{BB}) and dissimilar molecules (W_{AB}).

$$\chi = \frac{Z}{k_B T}\cdot(W_{AA} + W_{BB} - 2W_{AB}) \quad (1)$$

Here, χ is the interaction parameter, Z is the coordination number, k_B is the Boltzmann constant, and T is the temperature. In the total free energy, the direct interactions represented by the interaction parameter compete with the entropy of the system, so if the interaction energy W_{AA} or W_{BB} is similar to W_{AB}, no preferred interaction occurs ($\chi \approx 0$), and a statistical mixing is observed. The system of A and B tends to mix ($\chi < 0$) or phase-separate into the pure components ($\chi > 2$) if one of the interaction energy terms dominates. We emphasize that this is of course a simplified description. More complex scenarios involve the consideration of orientational order[55] and depth-dependent structural order in thin films.[56]

An overview of the mixing behavior for the PDI derivatives with DIP at high substrate temperature is shown in Figure 3. Regarding the different mixed systems, the equimolar films of PTCDI-C_1 ($PDIC_1$) and DIP do not form a cocrystal. Instead, the compounds tend to phase-separate. In the reciprocal space map in Figure 2f and the X-ray reflectivity scans (Figure S1) of the equimolar thin films, all visible peaks can be assigned to either pristine DIP or $PDIC_1$ domains. No new phase is observed even at a higher substrate temperature that should favor the mixing behavior.[9] Here, the energy term of the pure compounds seems to dominate ($W_{DIP/DIP} + W_{PDIC_1/PDIC_1} > 2\,W_{DIP/PDIC_1}$) because the lying-down conformation of the phase-separated $PDIC_1$[46] and the standing-up orientation of the phase-separated DIP[30,31,34] seem to be energetically more favorable than a cocrystal. Interestingly, a small amount of DIP domains with a lying-down conformation as well as a random orientation is also observed. A possible explanation for a lying-down conformation is that DIP domains which nucleate on top of already present $PDIC_1$ domains crystallize with their long molecular axis parallel to lying-down molecules of $PDIC_1$, while DIP crystallizes in the standing-up conformation on the silicon substrate.

A different picture arises for the mixing behavior of DIP and $PDIC_3$ deposited at a higher substrate temperature. The GIWAXS pattern (Figure 2g) shows a number of phases; however, none of them can be assigned to the pristine $PDIC_3$ shown in Figure 2b, suggesting the formation of a $PDIC_3$:DIP cocrystal. Two distinct cocrystal phases with a slightly different out-of-plane stacking can be distinguished based on the presence of two sets of peaks in the Q_z direction. Both phases of the cocrystals show a high degree of ordering and a well-defined thin film structure in both in-plane and out-of-plane directions as evidenced by the presence of pronounced reflection spots. This is in contrast to the thin film at room temperature, where DIP and $PDIC_3$ almost completely phase-separate (Figures S2 and S5g). Finally, several Debye−Scherrer ring features observed in the pattern can be attributed to a small amount of phase-separated DIP domains with a random orientation.[57−59] Here, the cocrystal formed partially overcomes the energy term of the pure compounds ($2\,W_{DIP/PDIC_3} > W_{DIP/DIP} + W_{PDIC_3/PDIC_3}$) which seems to be an energetically favorable orientation for both molecules.

The DIP:PTCDI-C_5 ($PDIC_5$) system is significantly more complex, as $PDIC_5$ is known to create numerous polymorphs when deposited at high substrate temperatures.[60] The reciprocal space map of pristine $PDIC_5$ (Figure 2c) shows reflections arising from three different unit cell structures consistent with previously observed polymorphs. This is in contrast to $PDIC_5$ deposited at room temperature (Figure S5c), where only one phase is observed. The reciprocal space map (Figure 2h) shows that $PDIC_5$ and DIP phase-separate. This observation is then confirmed by X-ray reflectivity scans (Figure S3). Most of the observed reflections arise from DIP domains with an exceptionally long-range ordering at both room and high substrate temperatures. This supports the observation that longer side chains promote higher crystallinity and therefore $W_{DIP/DIP} + W_{PDIC_5}/PDIC_5 > 2\,W_{DIP/PDIC_5}$. On the other hand, $PDIC_5$ reflections are barely visible and generally lack any preferential orientation. The only hint of a possible cocrystal formation is a set of weak but well-defined peaks at $Q_{xy} = 0.8$ and 1.28 Å^{-1}, that can not be attributed to any of the phases observed in the pristine films. It can be generally concluded that the attraction between similar molecules ($PDIC_5$) is larger.

Two different PDI derivatives with an n-octyl side chain are examined in this study, which differ in the cyano-groups in the imide position. Through the incorporation of this side group, the electron density of the aromatic backbone is reduced and the $\pi-\pi$ stacking is weaker due to steric hindrance of these side groups.[19,20,24,61] This leads to a lower crystallinity of the pure compound (Figure 2e) compared to the respective counterpart (Figure 2d). The mixing behavior of DIP and PTCDI-C_8 ($PDIC_8$) shows a complete phase-separation. Only peaks from both pure compounds are visible in the reciprocal space map of the equimolar thin film (Figure 2i), which are showing long-range ordering in the *xy*-direction and indicating a high crystallinity of the phase-separated pure compounds ($W_{DIP/DIP} + W_{PDIC_8/PDIC_8} > 2\,W_{DIP/PDIC_8}$). In comparison, the reciprocal space map of the equimolar mixed thin film of DIP and PTCDI-C_8-CN_2 ($PDIC_8$-CN_2) shows only reflections from a formed cocrystal (Figure 2j). No peaks from pristine DIP or $PDIC_8$-CN_2 are visible. This highlights a significant influence of the cyano-groups on packing and mixing behavior within these systems. Through the incorporated groups, the energy term $2\,W_{DIP/PDIC_8CN_2}$ becomes dominant compared to $W_{DIP/DIP} + W_{PDIC_8CN_2}/PDIC_8CN_2$, so that a cocrystal can be formed.

When comparing the different perylene diimide acceptors, the mixing behavior with DIP is strongly influenced by the structure of these molecules and therefore easily chemically tunable in the desired way. The different mixing behavior can also have an influence on the CT effects for the various thin film systems and will therefore be investigated by optical characterization methods.

https://doi.org/10.1021/acs.jpcc.2c07524
J. Phys. Chem. C 2023, 127, 11128−11137

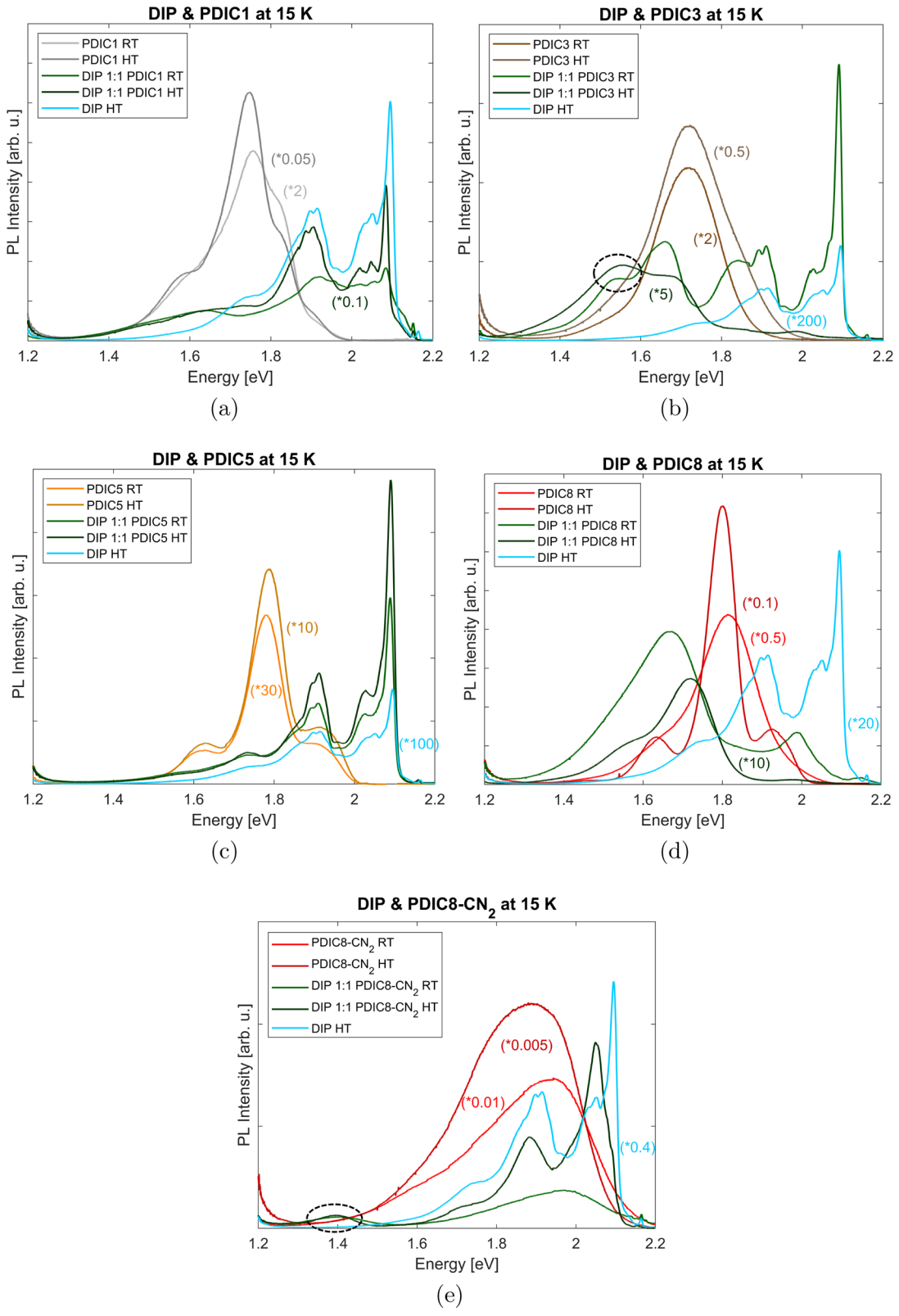

Figure 4. Photoluminescence spectra (measured at 15 K) of equimolar mixed films deposited at 25 and 150 °C: (a) DIP and $PDIC_1$, (b) DIP and $PDIC_3$, (c) DIP and $PDIC_5$, (d) DIP and $PDIC_8$, and (e) DIP and $PDIC_8$-CN_2 (CT peaks are marked in black). The spectra are scaled for clarity based on the respective equimolar mixed film grown at 25 °C and the signals at about 2.1 and 2.2 eV are background PL signals of the SiO_2 substrate.[62] Note that the apparent sharp peaks at 2.1 eV originate from the cutoff filter of the laser.

Optical Characterization. *Emission Data.* The various mixing scenarios observed for the DIP:PDI mixed films indicate that the alkyl chain variation should have a strong impact on charge transfer effects. To probe the influence of the structure and mixing scenario on the CT effects, we investigated the mixed

https://doi.org/10.1021/acs.jpcc.2c07524
J. Phys. Chem. C 2023, 127, 11128−11137

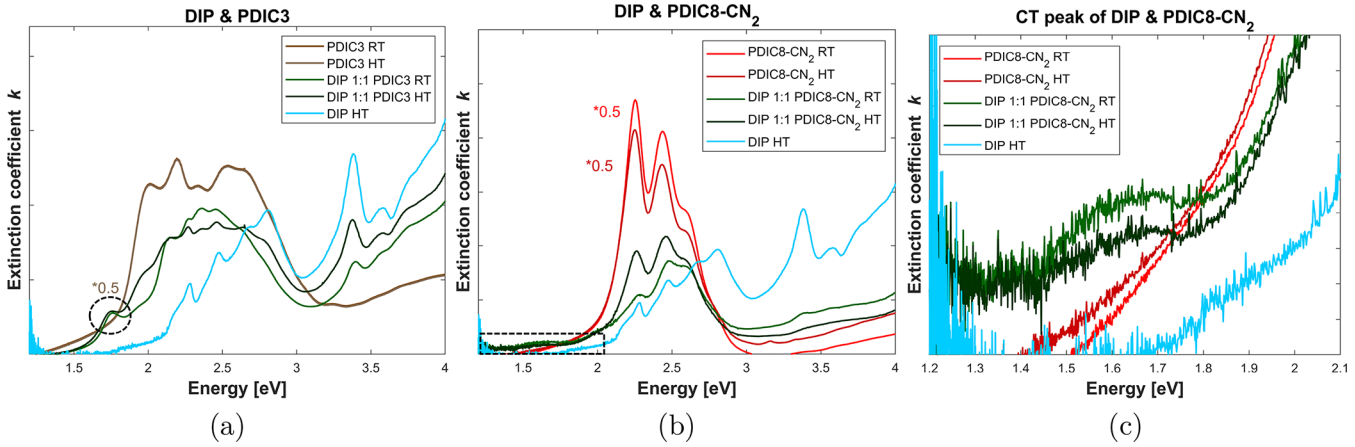

Figure 5. Absorption spectra of equimolar mixed films deposited at 25 and 150 °C: (a) DIP and $PDIC_3$ (CT peaks are marked in black), (b) DIP and $PDIC_8$-CN_2, and (c) enlarged section of the CT peak (black marked area of (b)). The spectra are scaled for clarity based on the respective equimolar mixed film grown at 25 °C.

thin films by emission and absorption spectroscopy. Figure 4 shows the emission spectra for the different DIP:PDI systems.

The emission features of the pure PDI derivatives vary only slightly. The temperature-dependent PL data for the pure PDI derivatives are shown in Figure S6. In Figure 4, the pure PDI emission spectra at a measurement temperature of 15 K are shown. For $PDIC_1$, $PDIC_5$, and $PDIC_8$ three dominant peaks are visible, which are sharper at low measuring temperatures. For $PDIC_3$ and $PDIC_8$-CN_2 only a broad emission feature is observed for all measurement temperatures. It is possible that for the PDIs with strong intermolecular interactions (high values of $W_{PDI/PDI}$) defined emission features are visible, whereas for the other compounds only one broad peak is observed.[63]

Regarding mixed films of DIP and $PDIC_1$, the photoluminescence spectra (Figure 4a) show for both equimolar films a broad peak at 1.6 eV which can be assigned to the pure acceptor molecule. The emission features of the equimolar films are superpositions of the two pure components DIP and $PDIC_1$. Donor−acceptor thin films of DIP and perylene diimide with an n-methyl alkyl chain cannot mix, forming no cocrystal and showing no CT effects.

Perylene diimide acceptor molecules with *n*-propyl chain favor the intermixing with the donor molecule DIP. In the emission spectra (Figure 4b), a peak at 1.70 eV originating from the pure $PDIC_3$ molecule and a peak at 1.55 eV assigned to the mixed cocrystal are visible for the equimolar thin films. This indicates that for DIP:$PDIC_3$ mixed films ES-CT effects occur in emission.

In the emission spectra (Figure 4c) of the $PDIC_5$:DIP system, peaks of the pure donor are well resolved for the equimolar thin films and there is only a small peak at 1.62 eV from the pure acceptor molecule. $PDIC_5$ and DIP show only limited intermixing with no degree of charge transfer presumably due to the higher attraction forces between similar $PDIC_5$ molecules. The system $PDIC_8$:DIP shows similar mixing behavior as $PDIC_5$:DIP and in the emission spectra (Figure 4d) also only peaks of the pure compounds are visible.

In contrast to DIP:$PDIC_8$, $PDIC_8$-CN_2, and DIP form a mixed cocrystal. In the emission spectra, there is a charge transfer peak for both DIP:$PDIC_8$-CN_2 equimolar thin films (Figure 4e). Here, we can see a peak maximum of the CT band at 1.33 eV for the film grown at room temperature and at 1.37 eV for the film prepared at higher substrate temperature. DIP and $PDIC_8$-CN_2 form an ordered mixed cocrystal with possibly two CT states.

In the next section, the absorption data for the various PDI:DIP thin film systems are investigated to achieve more insights into the different CT effects.

Absorption Data. Figure 5 shows the absorption spectra of the two perylene diimide systems mixed with the donor DIP which show charge transfer effects in the emission spectra (DIP:$PDIC_3$ and DIP:$PDIC_8$-CN_2). In the absorption spectra of the equimolar DIP:$PDIC_3$ thin films a sharp peak at 1.75 eV indicates a charge transfer effect between the donor and the acceptor molecule (Figure 5a). This CT peak is related to the PL peak at 1.55 eV. A shift in absorption to higher energy of ∼0.2 eV is common for related mixed systems.[43] A very broad CT band with an onset at 1.55 eV is visible for the equimolar thin films of DIP and $PDIC_8$-CN_2 (Figure 5c). For the mixed films of DIP:$PDIC_3$, a defined CT state is detectable, whereas for the $PDIC_8$-CN_2 and DIP, several CT states are observed as shown in the emission and in a broad band is visible in the absorption spectra.

Electroluminescence and Photocurrent Spectra. To complete the optical characterization regarding CT effects, we also measured electroluminescence (EL) and photocurrent spectra (expressed here as incident-photon-to-current efficiency (IPCE)) with the solar cell devices of DIP:$PDIC_3$ and DIP:$PDIC_8$-CN_2 mixture layers. For EL spectroscopy, the solar cell acts as LED by applying a forward voltage. Figure 6 shows the reduced EL and IPCE spectra for the two DIP:$PDIC_3$ and DIP:$PDIC_8$-CN_2 mixed layer devices on a logarithmic scale. The IPCE spectra correlate well with the absorption spectra for both equimolar thin films. The CT emission bands observed in the PL spectra for both systems are also visible in the two EL spectra, but, in contrast to the PL spectra, only a weak signal of the pristine materials (peak at 1.85 eV) can be observed in the DIP:$PDIC_3$ EL spectra, which indicates that nearly all injected electron−hole pairs recombine. We use the methodology introduced by Vandewal et al.[64] on adjustment for the crossing regime between reduced EL as well as the reduced IPCE spectra originating from CT states, following Marcus theory to estimate the CT energy E_{CT} in organic photovoltaic materials. For evaluation of the EL and IPCE spectra, the normalized reduced emission $\tilde{I}_{EL}(E)$ and absorption $\tilde{\eta}_{IPCE}(E)$ spectra, as defined in eqs 2 and 3, are fitted by Gaussian functions.[64,65] We note that in

https://doi.org/10.1021/acs.jpcc.2c07524
J. Phys. Chem. C 2023, 127, 11128−11137

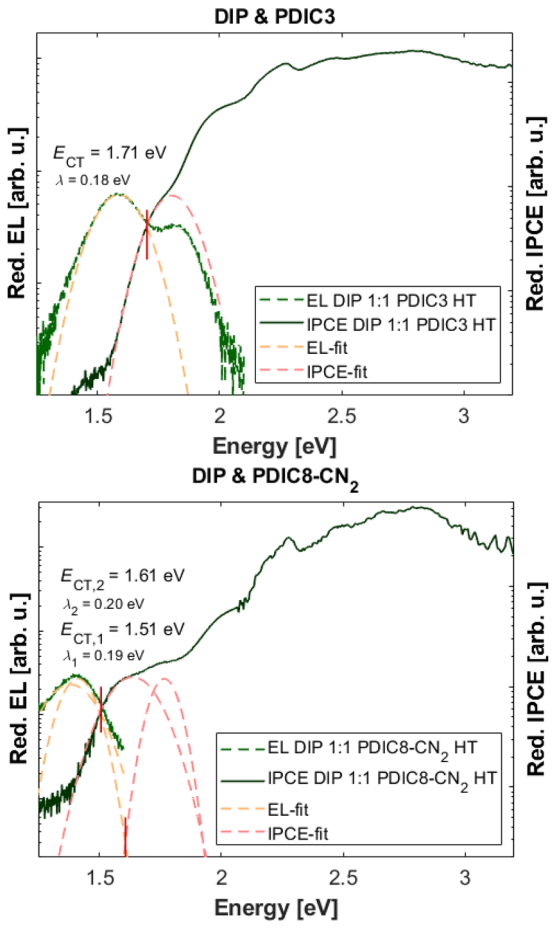

Figure 6. Reduced EL and IPCE spectra of DIP:$PDIC_3$ and DIP:$PDIC_8$-CN_2 mixed layer devices with the architecture ITO/HIL 1.3/organic mixed thin film (50 nm)/BCP (5 nm)/Al, with the respective Gaussian fits, the CT energies (marked by the red lines) as well as the λ parameters.

a recent theoretical work a different approach to the prefactors was presented,[66] but since most of the experimental work so far has used the expressions introduced by Vandewal et al., we prefer to stay with the latter in order to ensure comparability.

$$\tilde{I}_{EL}(E) \equiv \frac{I_{EL}(E)}{E} \propto \frac{1}{\sqrt{4\pi\lambda_{DA}k_BT}} \cdot \exp\left(-\frac{[E-(E_{CT}-\lambda_{DA})]^2}{4\lambda_{DA}k_BT}\right) \quad (2)$$

$$\tilde{\eta}_{IPCE}(E) \equiv \eta_{IPCE}(E)\cdot E \propto \frac{1}{\sqrt{4\pi\lambda_{DA}k_BT}} \cdot \exp\left(-\frac{[E-(E_{CT}+\lambda_{DA})]^2}{4\lambda_{DA}k_BT}\right) \quad (3)$$

Here, λ_{DA} represents the reorganization energy related to the Stokes shift in the CT manifold. The adiabatic CT energy is the crossing point of the fitted reduced EL and IPCE curves.[64−66] We obtain for the DIP:$PDIC_3$ system a CT energy of E_{CT} = 1.71 eV, in contrast to DIP:$PDIC_8$-CN_2, where we get two CT energies: $E_{CT,1}$ = 1.51 eV and $E_{CT,2}$ = 1.61 eV. When subtracting the λ parameters from the CT energies (crossing points), we receive the maxima of the EL curves. This yields an EL peak of 1.53 eV for DIP:$PDIC_3$, as well as 1.41 and 1.33 eV for the two EL peak energies of DIP:$PDIC_8$-CN_2, respectively. These values are in good agreement with the PL results where we also obtained one sharp CT state for DIP:$PDIC_3$ and two different CT peaks for the other DIP:PDI system. The performance of DIP:PDI mixed crystalline layers for photovoltaic device applications is generally limited by the upright standing orientation of the molecules. This leads to comparatively low light absorption under normal incidence. This is shown for DIP:$PDIC_3$ as well as DIP:$PIDC_8$-CN_2 in the Supporting Information (Figure S7). Furthermore, DIP:$PIDC_8$-CN_2 has the additional problem of a so-called S-shaped JV characteristics, which indicates a significant injection barrier for at least one carrier species.

In Figure 7 an overview of the excited-state CT effects for the different PDI derivatives is shown. Here, the CT energies are

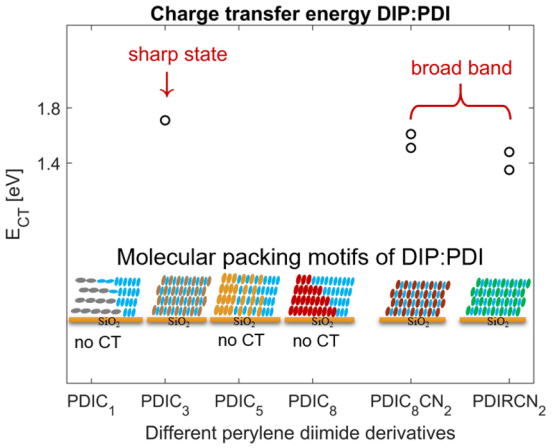

Figure 7. Schematic representation of the results for the ES-CT effects. The calculated CT energies by EL and IPCE data are presented for the different PDI derivatives with the respective CT peak features in the absorption data and the molecular packing motifs of the various DIP:PDI thin film systems.[8]

calculated based on EL and IPCE measurements for the different PDI derivatives and are presented with the resulting features in the absorption data. For the DIP:$PDIC_3$ system, the cocrystal formation leads to a sharp CT peak in absorption and a defined CT energy. In contrast, the DIP:$PDIC_8$-CN_2 mixed films show a broad CT band in absorption and two different CT energies. The 3-fold broadening of the Bragg peaks in the GIWAXS pattern of the DIP:$PDIC_8$-CN_2 equimolar films compared to the DIP:$PDIC_3$ system (see Figure 2g,j) might suggest more crystal defects in the equimolar thin films. Due to the higher disorder in the thin films, it is possible that more conformations from one molecule to nearest-neighbors can occur.[67] This could explain the various CT energies for the cocrystal phase of DIP and $PDIC_8$-CN_2.

The question arises, why DIP can only form a cocrystal with $PDIC_3$ and not with molecules with other chain lengths. Different factors play a role and influence the mixing behavior and charge transfer effects. What we can already qualitatively say is that a variation of the chain length of the side chains has two effects. First, the binding energy of the pure and the cocrystals probably increases, because the longer flexible side chains allow for various geometric conformations to maximize both the dense packing and a favorable quadrupole interaction with nearest neighbors. On the other hand, with increasing chain length, the size difference between donor (DIP) and acceptor ($PDIC_n$) increases, which is a hindrance for dense packing and therefore decreases the binding energy for a longer chain length. With this combination of the two effects, we find that only for $PDIC_3$ the binding energy of the cocrystal exceeds that of the two pure crystals.

https://doi.org/10.1021/acs.jpcc.2c07524
J. Phys. Chem. C 2023, 127, 11128−11137

CONCLUSIONS

In summary, we have performed a comprehensive study on mixing behavior and charge transfer effects of different donor−acceptor (DIP:PDI) molecular systems prepared by OMBD. The acceptor molecules differ in the *n*-alkyl side chain of the imide position and in the cyano groups of the bay position.

We found the optimized *n*-alkyl side chain length of the perylene diimide acceptors for the mixing behavior with DIP. With increasing chain length in the imide position of the acceptors, we found a strong CT effect as well as a strong mixing for the system DIP:$PDIC_3$ but not for molecules with longer side chains. $PDIC_3$ forms a well-defined cocrystal with DIP and shows a sharp ES-CT state.

Strong charge transfer and intermixing are also shown for systems of DIP and perylene diimide derivatives with cyano groups in the bay position. $PDIC_8$-CN_2:DIP forms also a well-ordered cocrystal, but with two ES-CT states. The incorporated cyano groups have an influence on the aromatic backbone of the perylene diimide derivatives and enable the formation of a cocrystal by reducing the binding energy of the pure ($PDIC_8$-CN_2) crystal.

Through the influence of the different side chains of the acceptor molecules on the mixing behavior and CT effects with DIP, it is possible to control mixing behavior and charge transfer effects using suitable perylene diimide molecules. A key to this is the structure of these acceptor molecules, which can be modified easily in the desired way.

ASSOCIATED CONTENT

Supporting Information

The Supporting Information is available free of charge at https://pubs.acs.org/doi/10.1021/acs.jpcc.2c07524.

XRR, additional GIWAXS, temperature-dependent PL data and JV-characteristic of the mixed thin films as well as additional unit cell parameters (PDF)

AUTHOR INFORMATION

Corresponding Authors

Alexander Hinderhofer − *Institut für Angewandte Physik, Universität Tübingen, 72076 Tübingen, Germany;* orcid.org/0000-0001-8152-6386; Email: alexander.hinderhofer@uni-tuebingen.de

Wolfgang Brütting − *Institut für Physik, Universität Augsburg, 86159 Augsburg, Germany;* orcid.org/0000-0001-9895-8281; Email: bruetting@physik.uni-augsburg.de

Frank Schreiber − *Institut für Angewandte Physik, Universität Tübingen, 72076 Tübingen, Germany; Center for Light-Matter Interaction, Sensors and Analytics LISA+, Universität Tübingen, 72076 Tübingen, Germany;* orcid.org/0000-0003-3659-6718; Email: frank.schreiber@uni-tuebingen.de

Authors

Nadine Rußegger − *Institut für Angewandte Physik, Universität Tübingen, 72076 Tübingen, Germany;* orcid.org/0000-0003-1746-4170

Hongwon Kim − *Institut für Physik, Universität Augsburg, 86159 Augsburg, Germany;* orcid.org/0000-0001-9600-8653

Jakub Hagara − *Institut für Angewandte Physik, Universität Tübingen, 72076 Tübingen, Germany;* orcid.org/0000-0002-7033-1783

Oleg Vladimirov − *Institut für Angewandte Physik, Universität Tübingen, 72076 Tübingen, Germany*

Timo Eberle − *Institut für Angewandte Physik, Universität Tübingen, 72076 Tübingen, Germany*

Ivan Zaluzhnyy − *Institut für Angewandte Physik, Universität Tübingen, 72076 Tübingen, Germany;* orcid.org/0000-0001-5946-2777

Alexander Gerlach − *Institut für Angewandte Physik, Universität Tübingen, 72076 Tübingen, Germany;* orcid.org/0000-0003-1787-1868

Complete contact information is available at: https://pubs.acs.org/10.1021/acs.jpcc.2c07524

Notes

The authors declare no competing financial interest.

ACKNOWLEDGMENTS

The authors gratefully acknowledge the financial support of the German Research Foundation (Deutsche Forschungsgemeinschaft, DFG), Project Number 239543752 (SCHR 700/20-2 and BR1728/14-2). We acknowledge DESY (Hamburg, Germany), a member of the Helmholtz Association HGF, for the provision of experimental facilities. Parts of this research were carried out at PETRA III, and we would like to thank Stephan Roth and Florian Bertram for assistance in using beamlines P03 and P08. The authors thank Jan Hagenlocher, Ekaterina Kneschaurek, Alessandro Greco, and Matthias Zwadlo for experimental help. We acknowledge LISA+ (Tüingen) for the provision of the CryoVac cooling system.

REFERENCES

(1) Tang, C. W. Two-Layer Organic Photovoltaic Cell. *Appl. Phys. Lett.* **1986**, *48*, 183−185.

(2) Brédas, J.-L.; Norton, J. E.; Cornil, J.; Coropceanu, V. Molecular Understanding of Organic Solar Cells: The Challenges. *Acc. Chem. Res.* **2009**, *42*, 1691−1699.

(3) Brütting, W., Ed. *Physics of Organic Semiconductors*; Wiley-VCH: Weinheim, 2005.

(4) Schwarze, M.; Schellhammer, K. S.; Ortstein, K.; Benduhn, J.; Gaul, C.; Hinderhofer, A.; Toro, L. P.; Scholz, R.; Kublitski, J.; Roland, S.; et al. Impact of Molecular Quadrupole Moments on the Energy Levels at Organic Heterojunctions. *Nat. Commun.* **2019**, *10*, 2466.

(5) Broch, K.; Dieterle, J.; Branchi, F.; Hestand, N. J.; Olivier, Y.; Tamura, H.; Cruz, C.; Nichols, V. M.; Hinderhofer, A.; Beljonne, D.; et al. Robust Singlet Fission in Pentacene Thin Films with Tuned Charge Transfer Interactions. *Nat. Commun.* **2018**, *9*, 954.

(6) Vandewal, K. Interfacial Charge Transfer States in Condensed Phase Systems. *Annu. Rev. Phys. Chem.* **2016**, *67*, 113−133.

(7) Vandewal, K.; Albrecht, S.; Hoke, E. T.; Graham, K. R.; Widmer, J.; Douglas, J. D.; Schubert, M.; Mateker, W. R.; Bloking, J. T.; Burkhard, G. F.; et al. Efficient Charge Generation by Relaxed Charge-Transfer States at Organic Interfaces. *Nat. Mater.* **2014**, *13*, 63−68.

(8) Belova, V.; Beyer, P.; Meister, E.; Linderl, T.; Halbich, M.-U.; Gerhard, M.; Schmidt, S.; Zechel, T.; Meisel, T.; Generalov, A. V.; et al. Evidence for Anisotropic Electronic Coupling of Charge Transfer States in Weakly Interacting Organic Semiconductor Mixtures. *J. Am. Chem. Soc.* **2017**, *139*, 8474−8486.

(9) Hinderhofer, A.; Schreiber, F. Organic-Organic Heterostructures: Concepts and Applications. *ChemPhysChem* **2012**, *13*, 628−643.

(10) Ruderer, M. A.; Müller-Buschbaum, P. Morphology of Polymer-Based Bulk Heterojunction Films for Organic Photovoltaics. *Soft Matter* **2011**, *7*, 5482−5493.

(11) Méndez, H.; Heimel, G.; Winkler, S.; Frisch, J.; Opitz, A.; Sauer, K.; Wegner, B.; Oehzelt, M.; Röthel, C.; Duhm, S.; et al. Charge-

Transfer Crystallites as Molecular Electrical Dopants. *Nat. Commun.* **2015**, *6*, 8560.
(12) Babuji, A.; Cazorla, A.; Solano, E.; Habenicht, C.; Kleemann, H.; Ocal, C.; Leo, K.; Barrena, E. Charge-Transfer Complexes in Organic Field-Effect Transistors: Superior Suitability for Surface Doping. *ACS Appl. Mater. Interfaces* **2022**, *14*, 44632−44641.
(13) Schweicher, G.; Garbay, G.; Jouclas, R.; Vibert, F.; Devaux, F.; Geerts, Y. H. Molecular Semiconductors for Logic Operations: Dead-End or Bright Future? *Adv. Mater.* **2020**, *32*, 1905909.
(14) Liscio, F.; Milita, S.; Albonetti, C.; D'Angelo, P.; Guagliardi, A.; Masciocchi, N.; Valle, R. G. D.; Venuti, E.; Brillante, A.; Biscarini, F. Structure and Morphology of PDI8-CN2 for n-Type Thin-Film Transistors. *Adv. Funct. Mater.* **2012**, *22*, 943−953.
(15) Rahimi, R.; Narang, V.; Korakakis, D. Optical and Morphological Studies of Thermally Evaporated PTCDI-C8 Thin Films for Organic Solar Cell Applications. *Int. J. Photoenergy* **2013**, *2013*, 1−7.
(16) Sugie, A.; Han, W.; Shioya, N.; Hasegawa, T.; Yoshida, H. Structure-Dependent Electron Affinities of Perylene Diimide-Based Acceptors. *J. Phys. Chem. C* **2020**, *124*, 9765−9773.
(17) Sun, Y.; Liu, Y.; Zhu, D. Advances in Organic Field-Effect Transistors. *J. Mater. Chem.* **2005**, *15*, 53−65.
(18) Molinari, A. S.; Alves, H.; Chen, Z.; Facchetti, A.; Morpurgo, A. F. High Electron Mobility in Vacuum and Ambient for PDIF-CN2 Single-Crystal Transistors. *J. Am. Chem. Soc.* **2009**, *131*, 2462−2463.
(19) Jones, B. A.; Facchetti, A.; Wasielewski, M. R.; Marks, T. J. Tuning Orbital Energetics in Arylene Diimide Semiconductors. Materials Design for Ambient Stability of n-Type Charge Transport. *J. Am. Chem. Soc.* **2007**, *129*, 15259−15278.
(20) Huang, C.; Barlow, S.; Marder, S. R. Perylene-3,4,9,10-tetracarboxylic Acid Diimides: Synthesis, Physical Properties, and Use in Organic Electronics. *J. Org. Chem.* **2011**, *76*, 2386−2407.
(21) Jung, B. J.; Tremblay, N. J.; Yeh, M.-L.; Katz, H. E. Molecular Design and Synthetic Approaches to Electron-Transporting Organic Transistor Semiconductors. *Chem. Mater.* **2011**, *23*, 568−582.
(22) Sun, J.-P.; Hendsbee, A. D.; Dobson, A. J.; Welch, G. C.; Hill, I. G. Perylene Diimide Based All Small-Molecule Organic Solar Cells: Impact of Branched-Alkyl Side Chains on Solubility, Photophysics, Self-Assembly, and Photovoltaic Parameters. *Org. Electron.* **2016**, *35*, 151−157.
(23) Jones, B. A.; Ahrens, M. J.; Yoon, M.-H.; Facchetti, A.; Marks, T. J.; Wasielewski, M. R. High-Mobility Air-Stable n-Type Semiconductors with Processing Versatility: Dicyanoperylene-3,4:9,10-bis(dicarboximides). *Angew. Chem., Int. Ed.* **2004**, *116*, 6523−6526.
(24) Pron, A.; Gawrys, P.; Zagorska, M.; Djurado, D.; Demadrille, R. Electroactive Materials for Organic Electronics: Preparation Strategies, Structural Aspects and Characterization Techniques. *Chem. Soc. Rev.* **2010**, *39*, 2577−2632.
(25) Rußegger, N.; Valencia, A. M.; Merten, L.; Zwadlo, M.; Duva, G.; Pithan, L.; Gerlach, A.; Hinderhofer, A.; Cocchi, C.; Schreiber, F. Molecular Charge Transfer Effects on Perylene Diimide Acceptor and Dinaphthothienothiophene Donor Systems. *J. Phys. Chem. C* **2022**, *126*, 4188−4198.
(26) Wang, C.; Wang, J.; Wu, N.; Xu, M.; Yang, X.; Lu, Y.; Zang, L. Donor−Acceptor Single Cocrystal of Coronene and Perylene Diimide: Molecular Self-Assembly and Charge-Transfer Photoluminescence. *RSC Adv.* **2017**, *7*, 2382−2387.
(27) Fan, H.; Shi, W.; Yu, X.; Yu, J. High Performance Nitrogen Dioxide Sensor Based on Organic Field-Effect Transistor Utilizing Ultrathin CuPc/PTCDI-C8 Heterojunction. *Synth. Met.* **2016**, *211*, 161−166.
(28) Aghamohammadi, M.; Fernández, A.; Schmidt, M.; Pérez-Rodríguez, A.; Goñi, A. R.; Fraxedas, J.; Sauthier, G.; Paradinas, M.; Ocal, C.; Barrena, E. Influence of the Relative Molecular Orientation on Interfacial Charge-Transfer Excitons at Donor/Acceptor Nanoscale Heterojunctions. *J. Phys. Chem. C* **2014**, *118*, 14833−14839.
(29) Huss-Hansen, M. K.; Hodas, M.; Mrkyvkova, N.; Hagara, J.; Nadazdy, P.; Sojkova, M.; Høegh, S. O.; Vlad, A.; Pandit, P.; Majkova, E.; et al. Early-Stage Growth Observations of Orientation-Controlled Vacuum-Deposited Naphthyl End-Capped Oligothiophenes. *Phys. Rev. Mater.* **2021**, *5*, 053402.
(30) Wagner, J.; Gruber, M.; Hinderhofer, A.; Wilke, A.; Bröker, B.; Frisch, J.; Amsalem, P.; Vollmer, A.; Opitz, A.; Koch, N.; et al. High Fill Factor and Open Circuit Voltage in Organic Photovoltaic Cells with Diindenoperylene as Donor Material. *Adv. Funct. Mater.* **2010**, *20*, 4295−4303.
(31) Gruber, M.; Rawolle, M.; Wagner, J.; Magerl, D.; Hörmann, U.; Perlich, J.; Roth, S. V.; Opitz, A.; Schreiber, F.; Müller-Buschbaum, P.; et al. Correlating Structure and Morphology to Device Performance of Molecular Organic Donor-Acceptor Photovoltaic Cells Based on Diindenoperylene (DIP) and C60. *Adv. Energy Mater.* **2013**, *3*, 1075−1083.
(32) Kowarik, S.; Gerlach, A.; Sellner, S.; Cavalcanti, L.; Konovalov, O.; Schreiber, F. Real-Time X-Ray Diffraction Measurements of Structural Dynamics and Polymorphism in Diindenoperylene Growth. *Appl. Phys. A: Mater. Sci. Process.* **2009**, *95*, 233−239.
(33) Heinemeyer, U.; Scholz, R.; Gisslen, L.; Alonso, M. I.; Osso, J. O.; Garriga, M.; Hinderhofer, A.; Kytka, M.; Kowarik, S.; Gerlach, A.; Schreiber, F. Exciton-Phonon Coupling in Diindenoperylene Thin Films. *Phys. Rev. B* **2008**, *78*, na.
(34) Dürr, A. C.; Schreiber, F.; Ritley, K. A.; Kruppa, V.; Krug, J.; Dosch, H.; Struth, B. Rapid Roughening in Thin Film Growth of an Organic Semiconductor (Diindenoperylene). *Phys. Rev. Lett.* **2003**, *90*, 016104.
(35) Heilig, M.; Domhan, M.; Port, H. Optical Properties and Morphology of Thin Diindenoperylene Films. *J. Lumin.* **2004**, *110*, 290−295.
(36) Kowarik, S.; Gerlach, A.; Schreiber, F. Organic Molecular Beam Deposition: Fundamentals, Growth Dynamics, and In Situ Studies. *J. Phys.: Condens. Matter* **2008**, *20*, 184005.
(37) Belova, V.; Hinderhofer, A.; Zeiser, C.; Storzer, T.; Rozbořil, J.; Hagenlocher, J.; Novák, J.; Gerlach, A.; Scholz, R.; Schreiber, F. Structure-Dependent Charge Transfer in Molecular Perylene-Based Donor/Acceptor Systems and Role of Side Chains. *J. Phys. Chem. C* **2020**, *124*, 11639−11651.
(38) Schreiber, F. Organic Molecular Beam Deposition: Growth Studies Beyond the First Monolayer. *Phys. Status Solidi A* **2004**, *201*, 1037−1054.
(39) Forrest, S. R. Ultrathin Organic Films Grown by Organic Molecular Beam Deposition and Related Techniques. *Chem. Rev.* **1997**, *97*, 1793−1896.
(40) Witte, G.; Wöll, C. Growth of Aromatic Molecules on Solid Substrates for Applications in Organic Electronics. *J. Mater. Res.* **2004**, *19*, 1889−1916.
(41) Björck, M.; Andersson, G. GenX: An Extensible X-Ray Reflectivity Refinement Program Utilizing Differential Evolution. *J. Appl. Crystallogr.* **2007**, *40*, 1174−1178.
(42) Parratt, L. G. Surface Studies of Solids by Total Reflection of X-Rays. *Phys. Rev.* **1954**, *95*, 359−369.
(43) Anger, F.; Ossó, J. O.; Heinemeyer, U.; Broch, K.; Scholz, R.; Gerlach, A.; Schreiber, F. Photoluminescence Spectroscopy of Pure Pentacene, Perfluoropentacene, and Mixed Thin Films. *J. Chem. Phys.* **2012**, *136*, 054701.
(44) Le, A. K.; Bender, J. A.; Arias, D. H.; Cotton, D. E.; Johnson, J. C.; Roberts, S. T. Singlet Fission Involves an Interplay between Energetic Driving Force and Electronic Coupling in Perylenediimide Films. *J. Am. Chem. Soc.* **2018**, *140*, 814−826.
(45) Ferguson, A. J.; Jones, T. S. Photophysics of PTCDA and Me-PTCDI Thin Films: Effects of Growth Temperature. *J. Phys. Chem. B* **2006**, *110*, 6891−6898.
(46) Yanagi, H.; Toda, Y.; Noguchi, T. Photoelectrochemical Behaviors of Orientation-Controlled Thin Films of N,N'-Substituted Perylene-3,4:9,10-bis(dicarboximide). *Jpn. J. Appl. Phys.* **1995**, *34*, 3808−3813.
(47) Petit, M.; Hayakawa, R.; Wakayama, Y.; Chikyow, T. Early Stage of Growth of a Perylene Diimide Derivative Thin Film Growth on Various Si(001) Substrates. *J. Phys. Chem. C* **2007**, *111*, 12747−12751.

https://doi.org/10.1021/acs.jpcc.2c07524
J. Phys. Chem. C 2023, 127, 11128−11137

(48) Krauss, T. N.; Barrena, E.; de Oteyza, D. G.; Zhang, X. N.; Major, J.; Dehm, V.; Würthner, F.; Dosch, H. X-ray/Atomic Force Microscopy Study of the Temperature-Dependent Multilayer Structure of PTCDI-C8 Films on SiO2. *J. Phys. Chem. C* **2009**, *113*, 4502−4506.
(49) Krauss, T. N.; Barrena, E.; Zhang, X. N.; de Oteyza, D. G.; Major, J.; Dehm, V.; Würthner, F.; Cavalcanti, L. P.; Dosch, H. Three-Dimensional Molecular Packing of Thin Organic Films of PTCDI-C8 Determined by Surface X-ray Diffraction. *Langmuir* **2008**, *24*, 12742−12744.
(50) Kam, A.; Aroca, R.; Duff, J.; Tripp, C. P. Evolution of the Molecular Organization in Bis(n-propylimido)perylene Films under Thermal Annealing. *Chem. Mater.* **1998**, *10*, 172−176.
(51) Kubozono, Y.; Hyodo, K.; Mori, H.; Hamao, S.; Goto, H.; Nishihara, Y. Transistor Application of New Picene-Type Molecules, 2,9-Dialkylated Phenanthro[1,2-b:8,7-b']dithiophenes. *J. Mater. Chem. C* **2015**, *3*, 2413−2421.
(52) Inokuchi, H.; Saito, G.; Wu, P.; Seki, K.; Tang, T. B.; Mori, T.; Imaeda, K.; Enoki, T.; Higuchi, Y.; Inaka, K.; et al. A Novel Type of Organic Semiconductors. Molecular Fastener. *Chem. Lett.* **1986**, *15*, 1263−1266.
(53) Kang, M. J.; Doi, I.; Mori, H.; Miyazaki, E.; Takimiya, K.; Ikeda, M.; Kuwabara, H. Alkylated Dinaphtho[2,3-b:2',3'-f]Thieno[3,2-b]Thiophenes (Cn-DNTTs): Organic Semiconductors for High-Performance Thin-Film Transistors. *Adv. Mater.* **2011**, *23*, 1222−1225.
(54) Inoue, S.; Minemawari, H.; Tsutsumi, J.; Chikamatsu, M.; Yamada, T.; Horiuchi, S.; Tanaka, M.; Kumai, R.; Yoneya, M.; Hasegawa, T. Effects of Substituted Alkyl Chain Length on Solution-Processable Layered Organic Semiconductor Crystals. *Chem. Mater.* **2015**, *27*, 3809−3812.
(55) Aufderheide, A.; Broch, K.; Novák, J.; Hinderhofer, A.; Nervo, R.; Gerlach, A.; Banerjee, R.; Schreiber, F. Mixing-Induced Anisotropic Correlations in Molecular Crystalline Systems. *Phys. Rev. Lett.* **2012**, *109*, 156102.
(56) Banerjee, R.; Novák, J.; Frank, C.; Lorch, C.; Hinderhofer, A.; Gerlach, A.; Schreiber, F. Evidence for Kinetically Limited Thickness Dependent Phase Separation in Organic Thin Film Blends. *Phys. Rev. Lett.* **2013**, *110*, 185506.
(57) Müller-Buschbaum, P. The Active Layer Morphology of Organic Solar Cells Probed with Grazing Incidence Scattering Techniques. *Adv. Mater.* **2014**, *26*, 7692−7709.
(58) Rivnay, J.; Mannsfeld, S. C. B.; Miller, C. E.; Salleo, A.; Toney, M. F. Quantitative Determination of Organic Semiconductor Microstructure from the Molecular to Device Scale. *Chem. Rev.* **2012**, *112*, 5488−5519.
(59) Chen, W.; Nikiforov, M. P.; Darling, S. B. Morphology Characterization in Organic and Hybrid Solar Cells. *Energy Environ. Sci.* **2012**, *5*, 8045−8074.
(60) Marin, F.; Tombolesi, S.; Salzillo, T.; Yaffe, O.; Maini, L. Thorough Investigation on the High-Temperature Polymorphism of Dipentyl-Perylenediimide: Thermal Expansion vs. Polymorphic Transition. *J. Mater. Chem. C* **2022**, *10*, 8089−8100.
(61) Barra, M.; Girolamo, F. V. D.; Chiarella, F.; Salluzzo, M.; Chen, Z.; Facchetti, A.; Anderson, L.; Cassinese, A. Transport Property and Charge Trap Comparison for N-Channel Perylene Diimide Transistors with Different Air-Stability. *J. Phys. Chem. C* **2010**, *114*, 20387−20393.
(62) Hummel, R. E.; Chang, S.-S. Novel Technique for Preparing Porous Silicon. *Appl. Phys. Lett.* **1992**, *61*, 1965−1967.
(63) Lifshitz, E.; Kaplan, A.; Ehrenfreund, E.; Meissner, D. Optical and Magnetooptical Measurements of N,N'-Dimethylperylene-3,4,9,10-tetracarboxylic Acid Diimide Thin Films. *J. Phys. Chem. B* **1998**, *102*, 967−973.
(64) Vandewal, K.; Benduhn, J.; Nikolis, V. C. How to Determine Optical Gaps and Voltage Losses in Organic Photovoltaic Materials. *Sustain. Energy Fuels* **2018**, *2*, 538−544.
(65) Linderl, T.; Zechel, T.; Hofmann, A.; Sato, T.; Shimizu, K.; Ishii, H.; Brütting, W. Crystalline versus Amorphous Donor-Acceptor Blends: Influence of Layer Morphology on the Charge-Transfer Density of States. *Phys. Rev. Appl.* **2020**, *13*, 024061.
(66) Coropceanu, V.; Chen, X.-K.; Wang, T.; Zheng, Z.; Brédas, J.-L. Charge-Transfer Electronic States in Organic Solar Cells. *Nat. Rev. Mater.* **2019**, *4*, 689−707.
(67) Huss-Hansen, M. K.; Kjelstrup-Hansen, J.; Knaapila, M. Structural Effects of Electrode Proximity in Vacuum-Deposited Organic Semiconductors Studied by Microfocused X-Ray Scattering. *Adv. Eng. Mater.* **2021**, *23*, 2100082.

https://doi.org/10.1021/acs.jpcc.2c07524
J. Phys. Chem. C 2023, 127, 11128−11137